CANCER GENOMICS & PROTEOMICS *1*: 407-418 (2004)

In Vivo and *In Vitro* Analysis of IL-10 in the NZB Leukemic Model

BRIAN A. McCARTHY[1], SIEW YEN CHONG[1], GEORGE PARKER[1], MONIQUE MERAMO[1], MING ZHANG[2], JENNIFER CZARNESKI[1], AMAL MANSOUR[1] and ELIZABETH RAVECHE[1]

[1]*New Jersey Medical School/UMDNJ, Newark, NJ;* [2]*Harvard Medical School, Boston, MA, U.S.A.*

Abstract. *Background: The B-1 malignancy, CLL has been associated with a failure to undergo apoptosis and increased endogenous IL-10 production. This study was undertaken to identify IL-10 effects in the NZB murine model of CLL. Materials and Methods: Antisense IL-10 was employed in vitro and in vivo to decrease IL-10 protein. Following treatment, cells were analyzed for alterations in cell cycle and RNA was studied for alterations in gene expression. Additional in vivo studies employed NZB mice in which the IL-10 gene was deleted. Results: IL-10 (-/-) knockout NZB mice overwhelmingly failed to develop leukemia. In vitro antisense IL-10 treatment resulted in a G2/M block and apoptosis and in vivo treatment with antisense IL-10 increased the survival of mice. Microarray analysis indicated a significant role for IL-10 in cell cycle regulation via cdc25C up-regulation and decreased p47^{phox} redox activity. Conclusion: In summary, IL-10 is a critical survival factor for malignant B cells via anti-apoptotic and cell cycle effects.*

CLL is characterized as a malignant expansion of B-1 cells, a subset of B cells which express features normally found on other hematopoietic cells, *i.e.* CD5 (T lymphocytes) and Mac-1/CD11b (macrophages) (1). B-1 cells are found predominantly in the peritoneum and clonal expansion of B-1 cells in the peritoneum has been implicated in CLL, the most common leukemia in the western world (2). B-1 cells compose a minor fraction of splenic B cells and are not normally present in lymph nodes. In contrast, they are the main B cell population in the peritoneal and pleural cavities. (1).

The role of IL-10 in cancer has been somewhat controversial. In one report, apoptosis was observed after treating B-CLL samples with IL-10 *in vitro* (3). Other laboratories have since found IL-10 in B-CLL samples and did not find IL-10 to be associated with apoptotic induction (4-7). Although initially termed "cytokine synthesis inhibitory factor" (CSIF) and characterized as a product of T helper 2 (Th2) cells that down-regulated interferon gamma in mice (8), IL-10 is now well known to have complex effects on many cell types (see review) (9). When analyzing CLL patients by ELISA, serum IL-10 levels were higher in CLL patients (median 5.04 pg/ml) than in normal volunteers (median undetectable, n=55) and increased IL-10 was an independent prognostic factor for decreased survival (10).

In order to examine the role of IL-10 in the protection of malignant cells from apoptosis, the NZB strain of mice, a murine model of CLL (2), was employed. Previous studies of the NZB have established that IL-10 is produced in an autocrine manner by the malignant B-1 cells in NZB (11-16). As a source of NZB malignant B-1 cells, an *in vitro* established line, LNC, (11) was used. LNC has previously been shown to express high levels of IL-10 and following *in vivo* transfer to result in a fatal B-1 malignant expansion. In contrast to wild-type, NZB IL-10 (-/-) knockout mice overwhelmingly fail to develop leukemic symptoms (12).

Microarray analysis of DNA can provide unprecedented clues into biological processes with great accuracy (17). Therefore, in this manuscript RNA was obtained from: untreated, antisense IL-10 or scrambled oligo-treated LNC, an NZB malignant B-1 cell line, and employed in microarray experiments. In this report, several new pathways influenced by IL-10 are elucidated.

Materials and Methods

Mice. NZB and BABL/c mice were obtained from Jackson Laboratory (Bar Harbor, ME, USA), and aged at the NJMS/UMDNJ research animal facility under specific pathogen-free conditions. Congenic NZB IL-10-deficient mice (IL-10 KO) were generated from IL-10 mice deficient on a C57BL/6 background (mice kind gift of Dr. Werner Muller, GBF Braunshweig, Germany) and backcrossed 8 times by speed congenics using a marker-assisted

Correspondence to: Dr. Elizabeth Raveche, UMDNJ -MSB C512, 185 South Orange Ave, Newark, NJ 07103, USA. Tel: 973-972-5240, Fax: 973-972-7293, e-mail: raveches@umdnj.edu

Key Words: CLL, IL-10, B-1 malignancy, antisense, microarray.

selection protocol for breeding (12). IL-10 KO mice were maintained by breeding heterozygous pairs to generate +/+, +/- and -/- progeny. IL-10-deficient mice were identified by DNA from tail clippings and RT-PCR for IL-10. NZB X DAB/1F1 mice (bred at NJMS) were used as recipients of NZB-derived B-1 malignant cells. Mice were employed at the indicated ages and, following the treatment outlined below, spleen and peritoneal cells (PWC) obtained.

Cell lines. LNC cells, an *in vitro* established line, obtained from the lymph node of a year old NZB mouse with CLL (11), were used as a source of malignant B-1 cells. HU-1 cells (fibroblastic) were obtained from the spleen of a 10-month-old IL-10 KO mouse and spleen cells from an age-matched NZB WT was used for the NZB-3 cell line. All *in vitro* cell lines were maintained in Iscove's modified Dulbecco's medium supplemented with 10% fetal calf serum, 200 mM L-glutamine and a 1% solution of penicillin, streptomycin and fungizone (Gibco BRL, Rockville, MD, USA). All experiments were performed with initial cell viability >90%.

Flow cytometry. Flow cytometry was used to detect surface marker expression, cell cycle changes and apoptosis. Cell cycle was detected by staining the DNA with propidium iodide (PI), (Calbiochem, San Diego, CA, USA). For PI staining, 1 x 10^6 cells were stained with hypotonic PI (0.05 mg/ml PI, 0.1%Triton X-100). FACS data were acquired on a Becton Dickinson FACS caliber with a 488-nm argon laser. Acquisition was done using CELLQuest software (Becton Dickinson, San Jose, CA, USA), and analysis was performed using ModFit LT software (Verity House Inc., Topsham, ME, USA). Apoptotic cells were calculated from the subG1 fraction as previously described (18). Additional apoptosis analysis employed double labeling with 1 μg/ml annexin-FITC (Caltag Lab, Burlinghame, CA, USA) and PI (isotonic) (19). In experiments involving *in vivo* treatment with IL-10, peritoneal lavage cells were obtained and stained with CD5-PE, CD19-APC and anti-BrdU-FITC. Fluorescein (FITC)-labeled antisense or scrambled oligonucleotides (see below) were employed to treat LNC at various concentrations for flow analysis of oligo uptake. Two μM FITC- treated LNC were used as a negative control. Cells were fixed in 2% paraformaldehyde and individual cells were analyzed for fluorescence by flow cytometry.

RT-PCR. Transcriptional determinations by reverse transcriptase polymerase chain reaction (RT-PCR) were made *via* RNA isolation (RNeasy mini-kit, Qiagen, Valencia, CA, USA). cDNA production was performed with Amplitaq Gold (Roche, Indianapolis, IN, USA). The primers were obtained from Operon (Alameda, CA, USA) or the UMDNJ Molecular Resource Facility, after a BLAST search and are as follows: IL-10 (5' CGGGAAGACAATAACTG 3' upstream), (5' ATTTCCGATAAGGCTTGG 3' downstream) and HPRT (5' GTTGGATACAGGCCAGACTTTGTTG 3' upstream), (5' GATT CAACTTGCGCTCATCTTAGGC 3' downstream). Following PCR reaction, the amplicons were electrophoresed, stained with ethidium bromide and analyzed with a fluorimager (Molecular Dynamics, Sunnyvale, CA, USA).

Antisense oligonucleotide treatment in vitro. Phosphorothioate derivitized oligonucleotides were synthesized by Operon (Alameda), and added to cells at a concentration of 20 μM. The IL-10 antisense sequence (ASN) was: (5' CATTTCCGATAAGGCTTGG 3') which binds to nucleotides 315-333 on the IL-10 mRNA (GenBank accession number M37897). For control oligonucleotides, scrambled sense was utilized: (SCR IL-10): (5' TTACTCGCTAAAGCGGTGT 3') The ASN IL-10 sequence has previously been shown to demonstrate an optimal decrease in IL-10 production *in vitro* (20).

IL-10 and antisense IL-10 in vivo treatment. BALB/c mice (age 4 months) were injected *i.p.* daily for 7 days with 200 μl (200 μg IL-10) of culture supernatant from P815 cells transfected with IL-10 or from P815 transfected with empty vector, as previously described (13). Four hours prior to obtaining peritoneal washout cells, the mice were injected with 100 μl of 10 mg/ml BrdU. For antisense studies, (NZB X DBA/2) mice (age 3 months) received an Alzet mini-osmotic pump (implanted *s.c.*) which delivered 300 μg/day of oligo for 4 weeks (pumps replaced with fresh oligo-containing pumps at 2 weeks) containing either antisense IL-10 or scrambled antisense. The mice received a transplantation of 20 x 10^6 LNC (*i.v.*) cells on the same day the pump was implanted. Transferred malignant B cells normally results in the *in vivo* expansion and death of the recipient at 30-45 days. Mice were killed when disease progression was apparent and survival day recorded and all aspects of humane animal use were reviewed and approved by IACUC.

Transmission electron microscopy. Cells were washed with PBS and pelleted. The cell pellet was resuspended in 2.5% gluteraldehyde and left for 1hour. The fixative was decanted, and the pellet was allowed to stand in 0.1M sodium phosphate buffer for 30 minutes. The buffer was decanted and the pellet was broken up into 1 mm pieces, which were cut in a Nova Ultrotome (LKB, Broma, Sweden) and mounted on 200 mesh copper grids, stained with a solution of 1% uranyl acetate/0.1% methanol, and examined according to standard procedures on a Philips 201 electron microscope.

Histological examination and image acquisition. Fresh frozen sections were cut into 5 micron sections, stained with Hematoxylin and Eosin (H&E) and gradually dehydrated until fixed in 100% xylene. Computerized images of H&E- stained glass slides were obtained using a Leica DM-RB compound microscope (Leica Microskopie und System Gmbh, Germany) with a 10x PL Fluotar lens and the "Image Pro Plus Version 4.0 for Windows" image processing and analysis system (Media Cybernetics, Silver Springs, MD, USA). Digitized images were acquired by a DEI CE color camera (Optronics, Goleta, CA, USA) and processed by a Microsoft NT Workstation on a Trinitron Pentium™ III computer. Optical images were obtained by adjusting the zoom, brightness sharpness and contrast to achieve optimal definition.

Gene chip analysis. Affymetrix gene chips for mice (U74A, Affymetrix, Santa Clara, CA, USA) were used to assay differential RNA expression between 24-hour treatment of AS IL-10, SS IL-10 and untreated LNC cells. The cRNAs were prepared from 12 μg of cytoplasmic RNA (RNeasy mini-kit, Qiagen) according to the manufacturer's instructions. Data was analyzed in Excel (Microsoft, Redmond, WA, USA). The original fold change data are stored in the NCBI microarray database (http://www.ncbi.nlm.nih.gov/geo/) as GSE1108. Genes were determined differentially expressed by antisense treatment if the Affymetrix analysis absolute call determined a difference, the fold change absolute value was greater than 2 when compared to untreated and the absolute value difference

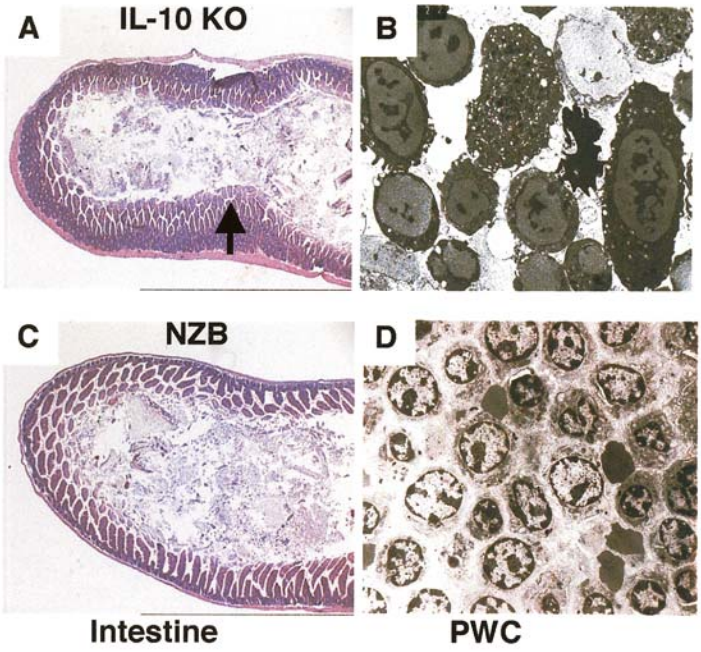

Figure 1. *IL-10 knockout mice. Histological examination of cells and tissue obtained from NZB IL-10 KO (upper panel) and NZB mice (lower panel). A and C, H&E stain of intestines show inflammation in the NZB IL-10 KO (-/-) but not an age-matched NZB. Arrow indicates cellular infiltration and inflammation. B and D, Analysis of pertioneal populations. Peritoneal cells from NZB IL-10 KO (-/-) and wild-type NZB were analyzed by transmission electron microscopy (TEM).*

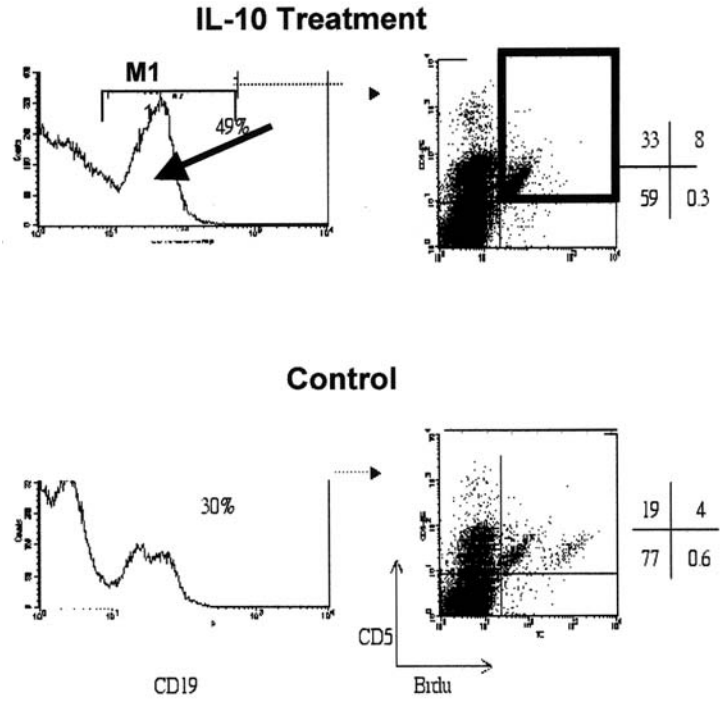

Figure 2. *In vivo IL-10. BABL/c mice were injected daily with 200 ng IL-10 (top panel) or control supernantant (bottom panel) followed by injection of BrdU (4 hours prior to lavage) and peritoneal washout cells were obtained on Day 7. Cells were stained with anti-CD19, anti-CD5 and anti-BrdU. Single histograms have markers to indicate CD19-positive population and arrow indicates increase in CD19 B cells following IL-10 treatment. Dual histograms are stained with CD5 (y axis) and BrdU (x axis). Box indicates cycling CD5-positive cells in the mice treated with IL-10. The numbers to the right are the percent of cells in each quadrant.*

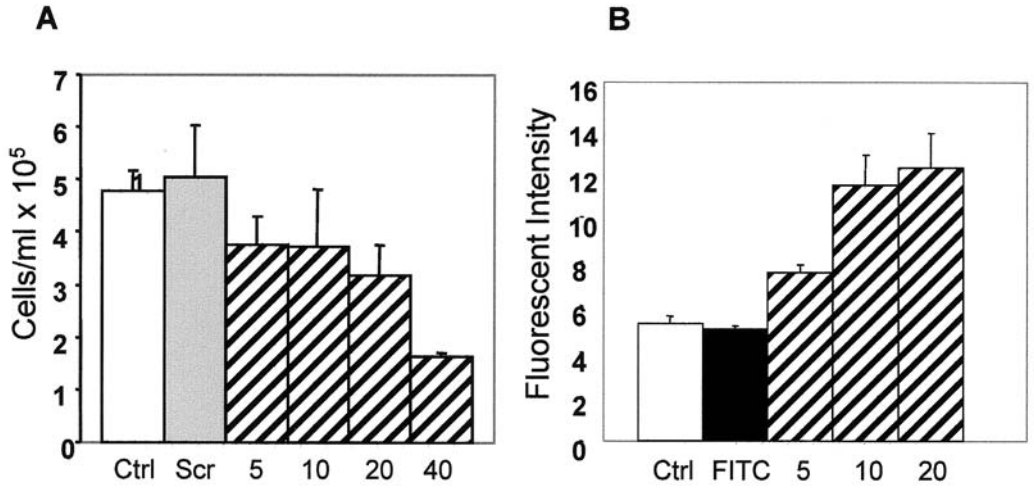

Figure 3. *Antisense IL-10 in vitro. (A) LNC cells were treated with varying doses of either scrambled (Scr) or antisense (Asn) IL-10 and assayed for cell number at 48 hours. The gray bar is scrambled sense as a negative control and hatched bars represent antisense treatment. X-axis represents μM of oligo treatment, y-axis is mean cell counts and error bars indicate standard errors of the mean. (B) FITC-labeled IL-10 antisense (5-20 μM) uptake by LNC as measured by flow cytometric analysis. X-axis represents μM of oligo treatment, y-axis is mean percent of highly fluorescent cells 24 hours post exposure to FITC-tagged oligonucleotides. FITC column (black bar) was treated with 2 μM FITC as a negative control, hatched bars represent antisense treatment.*

was greater than 2 when compared with scrambled oligo treatment. Information on each differential gene was obtained from Unigene (<http://www.ncbi.nlm.nih.gov/entrez/query.fcgi?db=unigene>). Pathway analysis was performed at the Affymetrix web site (www.affymetrix.com <http://www.affymetrix.com>) with the Gene Ontogeny Mining Tool (GO) (21, 22).

Results

Histological analysis of NZB and NZB IL-10 KO. Because IL-10 has been reported to be elevated in CLL, we investigated the impact of removing IL-10 in the NZB mouse model of this disease by creating NZB in which the IL-10 gene was knocked out (NZB IL-10 KO). Histological examination of the intestines from NZB and NZB IL-10 KO mice supports the known anti-inflammatory role for IL-10 in controlling inflammatory bowel disease (IBD). Similar to a previously reported analysis of intestines from mice devoid of IL-10 (23), the NZB IL-10 KO mice also had cellular infiltration in the intestines typical of an inflammatory process, indicated by the arrow (Figure 1A). In contrast, NZB, which develops auto-immunity and lymproliferative disease, had an apparently healthy intestine (Figure 1C).

To further analyze the role of IL-10 in the disease processes specific to NZB, the peritoneal lavage was analyzed. Peritoneal cells (PWC) from NZB IL-10 KO (-/-) were compared to NZB by transmission electron microscopy (TEM). NZB IL-10 KO peritoneal cells showed the presence of diverse cell types including macrophages and resting lymphocytes (Figure 1B). In contrast, NZB had a monotonous field of homogenous-appearing resting B cells (Figure 1D) characteristic of the clonal expansion of malignant B cells. In summary, microscopic examination clearly illustrated malignant B cell clonal expansion in the NZB, which was absent from the NZB IL-10 KO.

In vivo effects of IL-10 administration. Since previous reports had shown that B-1 cells produce and respond to IL-10 in CLL (4), we wished to investigate the effect of *in vivo* administration of IL-10 which might serve to increase B-1 cells in the peritoneum specifically. BABL/c mice were injected *i.p.* with IL-10 and the peritoneal wash examined for the presence of CD19- positive B cells. In addition, detection of *in vivo* dividing cells was accomplished by injection of BrdU to identify cells undergoing DNA replication. Mice that received IL-10 had increased numbers of B cells (Figure 2), which resulted in an increase in the number of peritoneal B cells following the administration of IL-10. The increase in CD5 dull BrdU+ cells was nearly double as well, indicating that exogenous administration of IL-10 increased the proliferation of peritoneal B-1 cells.

In vitro antisense IL-10 treatment. Based on the above results, IL-10 appears to play a pivotal role in the development of B-1 malignancy. We next investigated the effects of removing IL-10 in an already developed B-1 malignant cell. We have developed several techniques to reduce IL-10 levels including: antisense IL-10 oligonucleotides as well as RNAi oligos, which result in decreased IL-10 protein production.

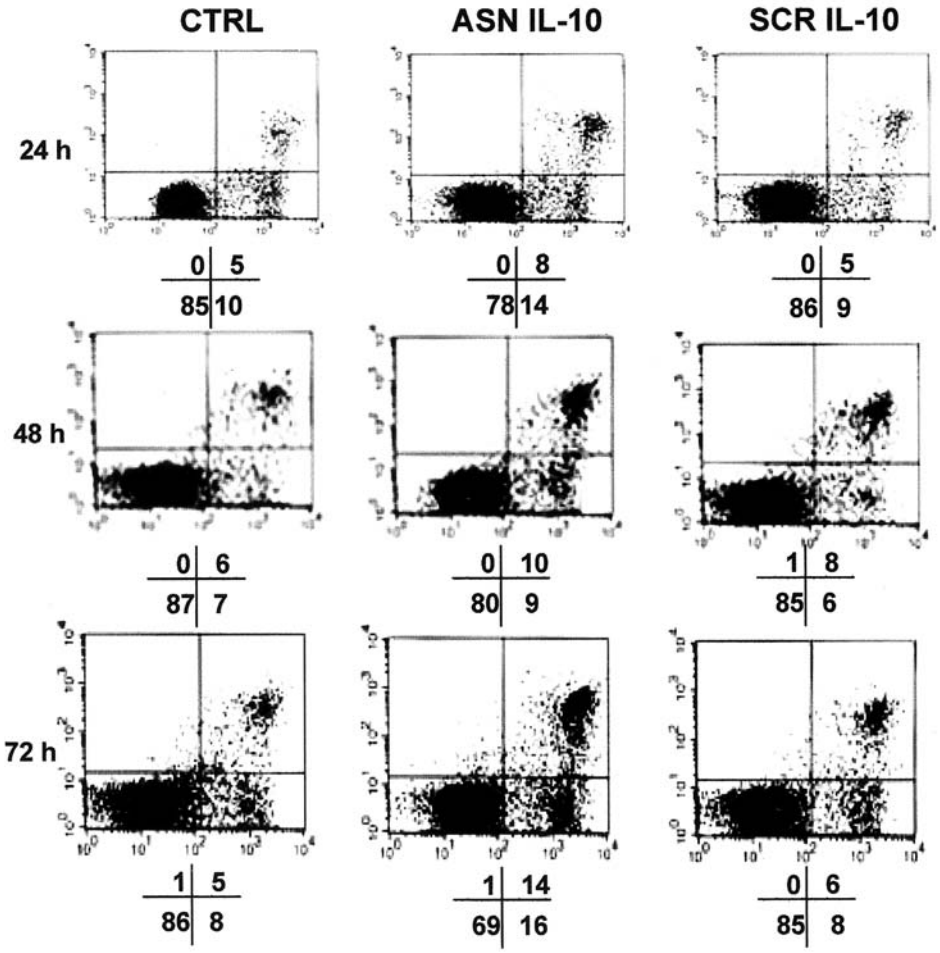

Figure 4. *Apoptosis induction by antisense IL-10 in vitro. LNC cells were either untreated or treated with antisense IL-10 or scrambled IL-10 oligonucleotides (20 μM) for the indicated times. Dual plots are Annexin (x-axis) and PI (y-axis) staining of LNC cells. Numbers represent the percent of the cells in each quadrant.*

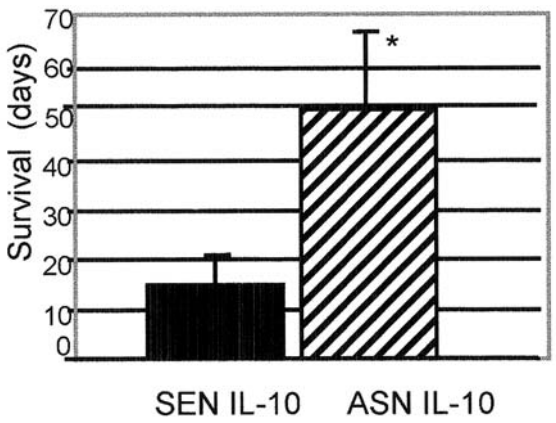

Figure 5. *In vivo survival with antisense IL-10. (NZB X DBA/2) F1 mice were implanted with a mini-osmotic pump (Alzet) containing either antisense IL-10 or scrambled antisense IL-10 oligonucleotides. The mice were transferred with 20 x 10^6 LNC cells. Columns represent the mean survival of mice and the bars represent the SEM. Approximately10 mice in each group.*

The antisense oligos act in a dose-dependent manner. LNC were treated with varying amounts of oligonucleotides and analyzed for cell growth. Antisense IL-10 treatment reduced cell growth in a dose-dependent manner (Figure 3A), whereas the scrambled sequence failed to inhibit proliferation. In order to examine the uptake of IL-10 antisense, FITC-labeled IL-10 antisense was employed at various doses. The uptake occurred in a dose-dependent manner (Figure 3B). Cells treated with 2 μM FITC were employed as negative controls. Based on these results, a concentration of 20 μM antisense IL-10 was employed to study the induction of apoptosis. Annexin V staining, which measures membrane changes indicative of early stage apoptosis, increased with time in cells treated with antisense IL-10 and this was not observed in the control oligo-treated cells (Figure 4). In addition to increased annexin staining, cells treated with antisense IL-10 had decreased proliferation and reduced cell counts (data not shown).

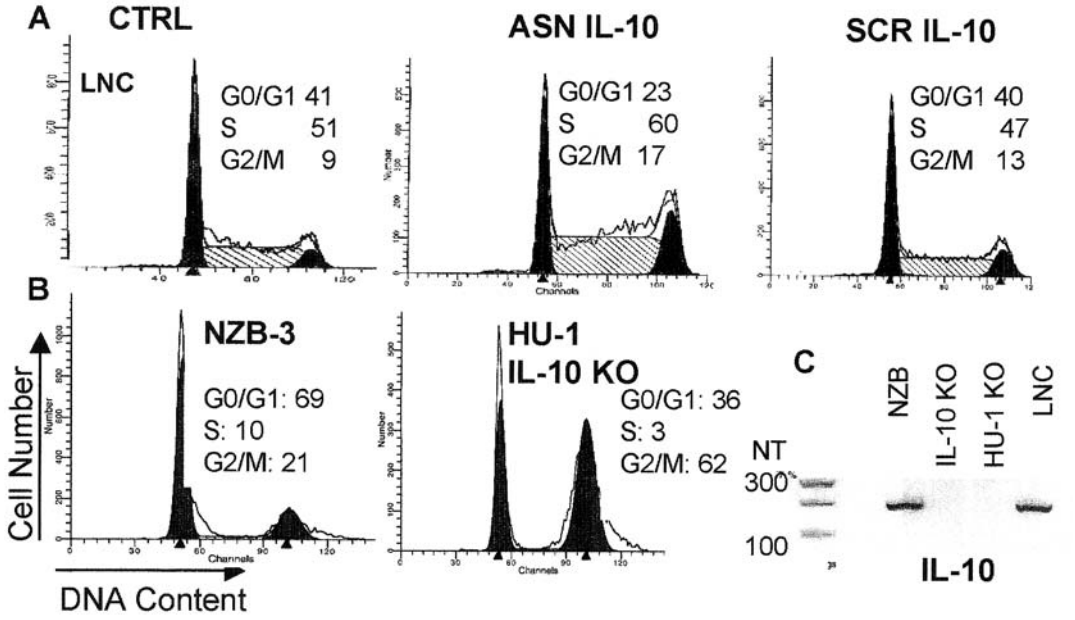

Figure 6. *Cell cycle effects of decreased IL-10. (A) LNC cells were cultured in media, antisense IL-10 or scrambled IL-10 for 24 hours and the cell cycle distribution determined with propidium iodide staining. (B) Cell cycle distribution following PI staining of Hu-1 cells obtained from 6-month cultures of NZB IL-10 spleen (the increased percent of cells in G2/M are indicated by arrow). For comparison, fibroblasts cultured from an age-matched WT NZB are shown. Numbers represent percent of cells in the cell cycle. PI graphs are representative of triplicate results. (C) RT-PCR analysis of IL-10 mRNA expression. NZB mice and LNC produced high levels of IL-10 (lanes 1 and 4) but none was detectable in the IL-10 KO spleen cells or the HU-1 cell line (lanes 2 and 3). The housekeeping gene HPRT had similar expression in each sample.*

Following *in vivo* treatment of already established malignant B-1 cell lines with antisense IL-10, the *in vivo* effects of antisense IL-10 were studied. Recipient (NZB X DBA/2) F1 mice were transferred with malignant B-1 cell lines, which grow in the recipient. Normally LNC cells will rapidly grow *in vivo* in the recipient mice resulting in death by Day 30. In contrast, mice which received mini-osmotic pumps delivering a constant amount of antisense IL-10 over a 28-day period survived twice as long as mice who did not receive the protective effects of antisense IL-10 (Figure 5).

IL-10-related alterations in cell cycle distribution. To determine the mechanism by which antisense IL-10 was anti-proliferative, studies of the cell cycle were performed. Blocking IL-10 has profound effects on the cell cycle distribution. Treatment of the NZB-derived malignant cell line, LNC with antisense IL-10 resulted in a G2/M block at 24 hours (Figure 6A). A similar block in G2/M was observed in cells derived from NZB IL-10 KO mice with no treatment. Splenic fibroblasts were obtained from mice with and without a functional gene encoding IL-10. Spleen cells, designated HU-1, from an NZB IL-10 KO mouse (verified by DNA analysis of the tail clipping) were cultured alongside an age-matched wild-type NZB (NZB-3) and by one month both cultures had a fibroblastic morphology. After 6 months, these cells were analyzed by PI staining for their cell cycle distribution (Figure 6B) and the lack of IL-10 in HU-1 cells was confirmed by RT-PCR. Both the LNC line treated with antisense IL-10 (Figure 6A) and the HU-1 devoid of IL-10 (Figure 6B) demonstrated an increased percentage of cells in the G2/M-phase of the cell cycle.

Microarray analysis of antisense IL-10-treated malignant B-1 cells. Analysis was performed to determine the gene expression regulated by IL-10. Microarray analysis was performed on the murine malignant B-1 cell line by comparing the effects of treatment with either antisense or scrambled IL-10 to untreated LNC. Scrambled oligo was used to control for the nonspecific effects of oligo administration. Antisense IL-10 treatment for 24 hours (a time which demonstrates a G2/M block but little apoptosis) influenced a limited number of genes out of the 12,000 tested and indicated a significant role for several genes in cell cycle regulation by IL-10, including the M-phase inducer phosphatase, cdc25C. After eliminating genes determined to have no change by Affymetrix difference call analysis, 48 genes with antisense IL-10 fold changes greater than 2 when compared to control and also different from scrambled (non-specific) by 2-fold (Asn-Scr) are graphically

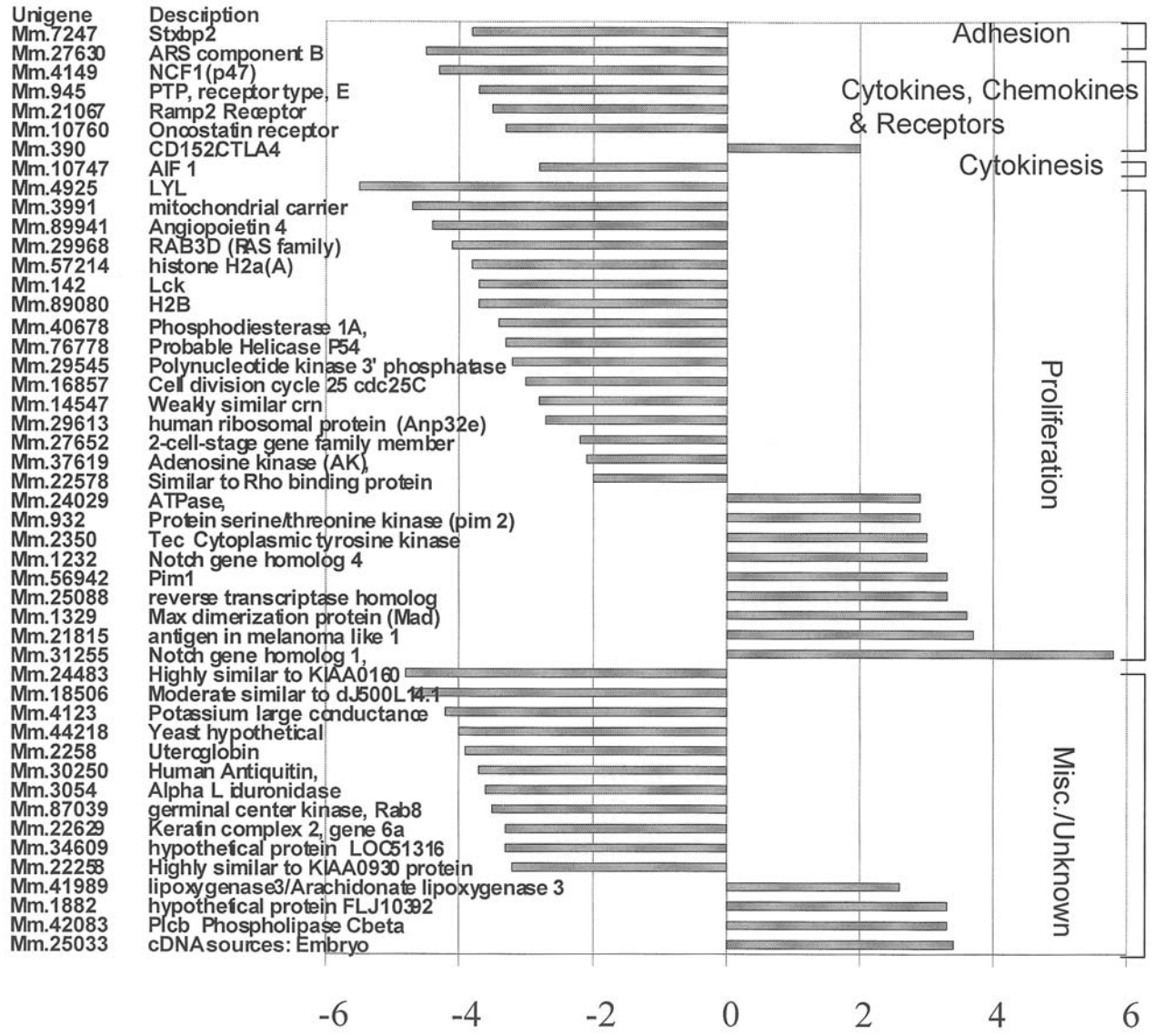

Figure 7. *Microarray analysis. IL-10 influenced a limited number of genes as detected by microarray analysis. Fold change in gene expression by microarray analysis is presented by horizontal bars. Forty-eight genes were determined different by computer analysis and caused a two-fold or greater change in LNC cells treated for 24 hours with antisense IL-10 when compared to both control and scrambled sense (to remove non-specific effects). Microarray analysis of samples sorts genes affected in the microarray of antisense IL-10 treatment, with a fold change greater than 2, by common groupings. Bars represent subtracting scrambled fold change from antisense fold change values.*

illustrated and the genes are divided into common groups (Figure 7). Of the limited number of genes affected by IL-10 removal, genes which regulate proliferation were the majority of the genes with altered expression in response to antisense IL-10 treatment when compared to both scrambled oligo treatment and untreated sources of RNA.

Systems analysis of the 48 differential genes was performed. The gene ontogeny mining tool (GO) sorts microarray results in a flow chart of related systems. Of the 48 genes passing our threshold, 21 were able to be analyzed by GO (Figure 8). An additional threshold of 2 probe sets was employed for inclusion in the lineage. Blocking IL-10 with antisense influenced several critical pathways including leukotriene metabolism, oxidoreductase activity, integral plasma membrane genes as well as both phosphorylation and dephosphorylation events. The regulation of selected nodes was analyzed quantitatively. Reducing IL-10 with antisense down-regulated 10 out of 13 genes identified as involved in cell growth and maintenance, 12 out of 19 metabolism genes and 6 out of 8 signal transduction genes.

Cell growth/ maintenance	
Ncf1/p47	-5.4
Cbx2	-4.4
D11Ertd530e	-3.5
Slc25a10	-3.3
Rab3d	-3.1
Kcnma1	-2.8
Stxbp2	-2.7
Krt2-6a	-2.2
Lck	-2.2
Cdc25c	-2
Plcb1	2.1
Notch1	3
Pim1	4.9

Cell proliferation	
Ncf1/p47	-5.4
Cdc25c	-2
Plcb1	2.1
Notch1	3

Cell cycle	
Cdc25c	-2
Plcb1	2.1

Receptor activity	
Osmr	-2
Notch1	3

Immune response	
Ncf1/p47	-5.4
Ctla4	3.2

Metabolism	
Ncf1/p47	-5.4
Lyl1	-4.5
Cbx2	-4.4
D11Ertd530e	-3.5
Adk	-3.4
Kcnma1	-2.8
Ptpre	-2.4
Aldh7a1	-2.4
Map4k3	-2.4
Idua	-2.3
Lck	-2.2
Cdc25c	-2
Plcb1	2.1
Mad	2.5
Notch1	3
Aloxe3	3.8
Pim2	4
Pim1	4.9
Tec	5.1

Fatty acid metab.	
Ncf1/p47	-5.4
Aloxe3	3.8

ATP binding	
Pnkp	-4.2
Map4k3	-2.4
Lck	-2.2
Notch1	3
Pim2	4
Pim1	4.9
Tec	5.1

Signal transduction	
Ncf1/p47	-5.4
Rab3d	-3.1
Ptpre	-2.4
Pde1a	-2.3
Lck	-2.2
Osmr	-2
Plcb1	2.1
Tec	5.1

Signal transducer	
1110021N19Rik	-3
Osmr	-2
Plcb1	2.1
Notch1	3

Transcription-DNA	
Lyl1	-4.5
Cbx2	-4.4
D11Ertd530e	-3.5
Mad	2.5
Notch1	3

Oxidoreductase	
Ncf1/p47	-5.4
Aldh7a1	-2.4
Aloxe3	3.8

Hydrolase activity	
Rab3d	-3.1
Ptpre	-2.4
Idua	-2.3
Pde1a	-2.3
Cdc25c	-2
Plcb1	2.1

Phosphoric diester hydrolase activity	
Pde1a	-2.3
Plcb1	2.1

Kinase activity	
Pnkp	-4.2
Adk	-3.4
Map4k3	-2.4
Lck	-2.2
Pim2	4
Pim1	4.9
Tec	5.1

Protein tyrosine phoshatase activity	
Ptpre	-2.4
Cdc25c	-2

Protein tyrosine kinase activity	
Map4k3	-2.4
Lck	-2.2
Pim1	4.9
Tec	5.1

Serine/threonine kinase activity	
Map4k3	-2.4
Lck	-2.2
Pim2	4
Pim1	4.9
Tec	5.1

Figure 8. *Microarray gene ontogeny analysis. (A) Quantitative analysis of selected GO nodes. Major pathways determined from microarray analysis by the gene ontogeny mining tool (bold print) are listed in order of fold change from the most down-regulated.*

Discussion

IL-10 has been termed "the most relevant cytokine for B cell survival both in mice and humans" (24) and is the subject of intense investigation (25). B-1 cells are the major producers of antibodies *in vivo* as well as the major producer of B cell -derived IL-10 (26). In the present study we found that IL-10 had cell cycle regulation, anti-apoptotic effects and protected malignant B-1 cells from death both *in vitro* and *in vivo*. Evidence is presented here that IL-10 plays an important role in the maintenance of malignant B-1 cells through analysis of NZB IL-10 KO mice as well as *in vitro* and *in vivo* studies involving blockage of IL-10 *via* antisense. To further examine the pathways and genes involved in IL-10-mediated growth, microarray analysis was performed.

IL-10 sustains the growth of activated B cells (27), promotes the differentiation of B cells into plasma cells (28-30) and is involved in the development of AIDs-related B lymphoma as an autocrine growth factor (31). CLL, the most common leukemia in the western world, results from an expansion of B-1 cells. The NZB mice develop CLL with malignant B-1 cells present in blood, bone marrow, spleen and peritoneum. In this report, normal non-NZB mice injected with exogenous IL-10 had increased growth of peritoneal B-1 cells, suggesting that IL-10 may be critical for the development of B-1 malignant disease. In keeping with

this, NZB mice devoid of IL-10 failed to develop B-1 malignant clones and electron microscopic analysis of peritoneal cells demonstrated a monotonous expansion of malignant B cells in the NZB but not the NZB IL-10 KO.

Antisense IL-10 *in vivo* has been shown by this laboratory to efficiently decrease IL-10 protein levels, as measured by ELISA (20, 32). Decreasing IL-10 by antisense IL-10 resulted in apoptosis induction and profound effects on the cell cycle in NZB-derived B-1 malignant cells, resulting in a G2/M arrest. In our antisense IL-10 microarray analysis, IL-10 was found to affect a limited number of genes. Microarray analysis of the NZB mouse model parallels human CLL microarrays (33). In addition to several known leukemia genes (Lyl, Lck, cdc25C) down-regulated by antisense IL-10, novel mechanisms in the role of IL-10 are identified.

IL-10 signals through tyrosine kinase, resulting in phosphorylation of STAT1 and STAT3 (34). STAT 3 has been implicated in the prevention of apoptosis (35, 36) and found to be differentially expressed in normal, self-renewing B-1 cells when compared to conventional B lymphocytes (37). In the present manuscript, microarray analysis *via* gene ontology analysis of pathways altered by IL-10 antisense revealed tyrosine phosphorylation to be a gene family involved. Oncogenes/oncoproteins turned down by ASN IL-10 included Lyl, known to be involved in the NFÎ B pathway of some T cell acute leukemias (38), Rab3d, a member of the Ras oncogene family (39), Map kinase kinase kinase kinase 3 (Map4k3) and the lymphocyte cell kinase (Lck) which interacts with cdc2 (40). Interestingly the strong proto-oncogene PIM1 and its structural homolog PIM2, known to collaborate with myc (41), were turned up following antisense IL-10 treatment. Notch 1 expression was increased in malignant B cells following antisense IL-10, which may have a profound effect *in vivo*. Notch 1 has been shown to increase the ratio of CD8 to CD4 single positive thymocytes (42) and, since IL-10 is known to down-regulate Th1-CTL responses, an increase could be expected after IL-10 removal.

Advances in systems biology allow pathway analysis of microarrays by biologic process, molecular function and cellular component. Such analysis indicated metabolism (n=19) and cell growth (n=13) were the largest pathways affected in cellular and physiologic processes after antisense IL-10 treatment. Cell cycle regulators were identified by microarray analysis; cdc25C was reduced and phospholipase C beta1 (Plcb1) increased by antisense IL-10. The nuclear form of Plcb1 has been shown to be key in the regulation of mitogen-induced cell growth and normally speeds the progression of cells through G1 (43). The significance of an antisense IL-10-induced increase in Plcb1 is not clear but perhaps contributes further to the stall in G2/M following antisense IL-10 treatment. Alternatively, postulating that IL-10 normally speeds the progression of malignant B cells through G2/M, low levels of Plcb1 (increased by antisense), are consistent with high levels of p27, (reduced by antisense). The cell cycle regulator, cdc25C, an M-phase inducer phosphatase elevated in murine CLL, was decreased by antisense IL-10, consistent with two previous CLL microarrays (44, 45), which found elevated cdc25 in CLL. Taken together, this suggests an upstream role for IL-10, through cdc25C regulation, in the pivotal cellular decision to divide.

Two genes decreased in our antisense IL-10 microarray involving adenosine (murine adenosine kinase and adenine nucleotide translocator) are of interest since adenosine receptor agonists have been shown to differentially regulate IL-10 during hypoxia (oxygen deficiency) and accumulation of intracellular adenosine has been associated with increased levels of IL-10 (46). Another gene decreased by antisense IL-10 was $p47^{phox}$, a component of the phagocyte NADPH oxidase pathway, which enhances superoxide production (47) and a defect in this is implicated in granulomatous disease (48) and inflammatory bowel disease (IBD) (49). In addition, Epstein-Barr virus, which has a viral IL-10 homolog, transforms B cells, increases IL-10 and induces the expression of phagocyte NADPH oxidase, $p47^{phox}$ protein (50-51). The microarray data suggest dual attack/defense mechanisms where malignant B cells achieve an advantage through the stimulation of oxidative stress and redox reactions have been shown in human CLL (52). In summary, the antisense IL-10 microarray identified genes previously known to be involved in CLL and revealed new genes and pathways involved in CLL: a) oncogenes Bcl7C b) proliferation cdc25C c) inflammation/activation $p47^{phox}$.

Finally, two independent methods were used in this report to decrease IL-10: antisense and knockout mice. In response to treatment with IL-10 antisense, malignant B-1 cells underwent apoptosis, a G2/M cell cycle block as well as decreased levels of IL-10 and cdc25C. The IL-10 KO mice on an NZB background failed to develop any substantial symptoms of B-1 leukemia, observable in the normal aging process of wild-type NZB. These data strongly suggest blocking IL-10 may have clinical value, either alone or in combination therapy, to treat certain B cell leukemias.

Acknowledgements

This work was supported by grants from the National Institute of Health and the New Jersey Commission on Cancer Research, U.S.A.

Grateful appreciation to T. Jones, C. Fernandez and T.K. Vaidyanathan for their technical expertise. This work is in partial fulfillment of the Ph.D. thesis of Brian McCarthy, Department of Experimental Pathology and Laboratory Medicine, GSBS-UMDNJ.

References

1 Abrahao TB, Freymuller E, Mortara RA, Lopes JD and Mariano M: Morphological characterization of mouse B-1 cells. Immunobiology *208*: 401-411, 2003.

2 Phillips JA, Mehta K, Fernandez C and Raveche ES: The NZB mouse as a model for chronic lymphocytic leukemia. Cancer Res *52*: 437-443, 1992.

3 Fluckiger A, Durand I and Banchereau J: IL-10 induces apoptotic cell death of B-CLL. J Exp Med *179*: 91-99, 1994.

4 Jurlander J *et al*: IL-10 is a survival factor for B-CLL. Blood *86*: 1372, 1995.

5 Morabito F, Filangeri M, Sculli G and Oliva B: *In vitro* modulation of bcl-2 protein expression, drug induced apoptosis and cytotoxicity by IL-10 in CLL. Haematologica *83*: 1046-1048, 1998.

6 Knauf WU, Ehlers B, Bisson S and Thiel E: Serum levels of IL-10 in B-CLL. Blood *86*: 4382-4386, 1995.

7 Kamper E *et al*: Serum levels of tetranectin, ICAM-1 and IL-10 in CLL. Clin Biochem *32*: 639-645, 1999.

8 Fiorentino DF, Bond MW and Mosmann TR: Two types of mouse T helper cell. IV. Th2 clones secrete a factor that inhibits cytokine production by Th1 clones. J Exp Med *170*: 2081-2095, 1989.

9 Pestka S, Krause CD, Sarkar D, Walter MR, Shi Y and Fisher PB: Interleukin-10 and related cytokines and receptors. Ann Rev Immunol *22*: 929-979, 2004.

10 Fayad L *et al*: IL-6 and IL-10 levels in CLL: correlation with phenotypic characteristics and outcome. Blood *97*: 256-263, 2001.

11 Peng B, Sherr DH, Mahboudi F, Hardin J, Sharer L and Raveche ES: A cultured malignant B-1 line serves as a model for Richter's syndrome. J Immunol *19*: 159-167, 1994.

12 Czarneski J *et al*: Studies in NZB IL-10 knockout mice of the requirement of IL-10 for progression of B-cell lymphoma. Leukemia *18*: 597-606 2004.

13 Parker G, Peng B, He M, Gould-Fogerite S, Chou C and Raveche ES: *In vivo* and *in vitro* antiproliferative effects of antisense interleukin 10 oligonucleotides. Methods Enzymol *314*: 411-429, 2000.

14 Ramachandra S, Metcalf RA, Fredrickson T, Marti GE and Raveche ES: Requirement for increased IL-10 in the development of B-1 lymphoproliferative disease in a murine model of CLL. J Clin Invest *98*: 1788-1793, 1996.

15 Chong S *et al*: Cell cycle effects of IL-10 on malignant B-1 cells. Genes Immunity *2*: 239-247, 2001.

16 McCarthy BA, Mansour A, Lin YC, Kotenko S and Raveche ES: RNA interference of IL-10 in leukemic B-1 cells. Cancer Immunity *4*: 6, 2004.

17 Leung YF and Cavalieri D: Fundamentals of cDNA microarray data analysis. Trends Genet *19*: 649-59, 2003.

18 Nicoletti I, Migliorati G, Pagliacci M, Grignani F and Riccardi C: A rapid simple method for measuring thymocyte apoptosis by propidium iodide staining and flow cytometry. J Immunol Meth *139*: 271-279, 1991.

19 Koopman G, Reutelingsperger CP, Kuijten GAM, Keehnen RMJ, Pals ST and van Oers MHJ: Annexin V for flow cytometric detection of phosphatidylserine expression on B cells undergoing apoptosis. Blood *84*: 1415-1420, 1994.

20 Peng B, Mehta NH, Fernandes H, Chou CC and Raveche ES: Growth inhibition of malignant CD5+B (B-1) cells by antisense IL-10 oligonucleotide. Leukemia Res *19*: 159-167, 1995.

21 Liu G *et al*: NetAffx: Affymetrix probesets and annotations. Nucleic Acids Res *31*: 82-86, 2003.

22 Ashburner M *et al*: Gene ontology: tool for the unification of biology. The Gene Ontology Consortium. Nat Genet *25*: 25-29, 2000.

23 Kuhn R, Lohler J, Rennick D, Rejewsky K and Muller W: Interleukin-10-deficient mice develop chronic enterocolitis. Cell *75*: 263-274, 1993.

24 Gary-Gouy H, Harriague J, Bismuth G, Platzer C, Schmit C and Dalloul A: Human CD5 promotes B cell survival through stimulation of autoctrine IL-10 production. Blood *100*: 4537-4543, 2002.

25 Benjamin D, Park CD and Sharma V: Human B cell interleukin 10. Leuk Lymphoma *12*: 205-210, 1994.

26 O'Garra A, Chang R, Go N, Hastings R, Haughton G and Howard M: Ly-1 B (B-1) cells are the main source of B cell-derived interleukin 10. Eur J Immunol *22*: 711-717, 1992.

27 Rousset F *et al*: Interleukin 10 is a potent growth and differentiation factor for activated human B lymphocytes. Proc Natl Acad Sci USA *89*: 1890-1893, 1992.

28 Kobayashi N, Nagumo H and Agematsu K: IL-10 enhances B-cell IgE synthesis by promoting differentiation into plasma cells, a process that is inhibited by CD27/CD70 interaction. Clin Exp Immunol *129*: 446-452, 2002.

29 Rousset F *et al*: Long-term cultured CD40-activated B lymphocytes differentiate into plasma cells in response to IL-10 but not IL-4. Int Immunol *7*: 1243-53, 1995.

30 Agematsu K, Hokibara S, Nagumo H, Shinozaki K, Yamada S and Komiyama A: Plasma cell generation from B-lymphocytes *via* CD27/CD70 interaction. Leuk Lymphoma *35*: 219-225, 1999.

31 Masood R *et al*: IL-10 is an autocrine growth factor for acquired immunodeficiency syndrome-related B cell lymphoma. Blood *85*: 3423-3430, 1995.

32 Parker G *et al*: Antisense IL-10 abrogrates the inhibitory effects of IL-10 production by transfected tumor cells. Cytokines Cell Mol Therapy *6*: 6113-6119, 2000.

33 Alizadeh A *et al*: Distinct types of diffuse large B-cell lymphoma identified by gene expression profiling. Nature *403*: 503-511, 2000.

34 Finbloom DS and Winestock KD: IL-10 induces the tyrosine phosphorylation of tyk2 and Jak1 and the differential assembly of STAT1 alpha and STAT3 complexes in human T cells and monocytes. J Immunol *155*: 1079-1090, 1995.

35 Alas S and Bonavida B: Inhibition of constitutive STAT3 activity sensitizes resistant non-Hodgkin's lymphoma and multiple myeloma to chemotherapeutic drug-mediated apoptosis. Clin Canc Res *9*: 316-326, 2003.

36 Fukada T *et al*: Two signals are necessary for cell proliferation induced by a cytokine receptor gp130: involvement of STAT3 in anti-apoptosis. Immunity *5*: 449-460, 1996.

37 Karras J, Wang Z, Huo L, Howard R, Frank D and Rothstein TL: Signal transducer and activator of transcription-3 (STAT3) is constitutively activated in normal, self-renewing B-1 cells but only inducibly expressed in conventional B lymphocytes. J Exp Med *185*: 1035-1042, 1997.

38 Ferrier R, Nougarede R, Doucet S, Kahn-Perles B, Imbert J and Mathieu-Mahul D: Physical interaction of the bHLH LYL1 protein and NF-kappaB1 p105. Oncogene *18*: 995-1005, 1999.

39 Roa M, Paumet F, Le Mao J, David B and Blank U: Involvement of the ras-like GTPase rab3d in RBL-2H3 mast cell exocytosis following stimulation *via* high affinity IgE receptors (Fc epsilonRI). J Immunol *159*: 2815-2823, 1997.
40 Pathan NI, Geahlen RL and Harrison ML: The protein-tyrosine kinase Lck associates with and is phosphorylated by Cdc2. J Biol Chem *271*: 27517-27523, 1996.
41 van der Lugt N *et al*: Proviral tagging in E mu-myc transgenic mice lacking the Pim-1 proto-oncogene leads to compensatory activation of Pim-2. EMBO J *14*: 2536-2544, 1995.
42 von Boehmer H: Coming to grips with notch. J Exp Med *194*: F43-46, 2001.
43 Peruzzi D *et al*: Molecular characterization of the human PLC beta1 gene. Biochim Biophys Acta *1584*: 46-54, 2002.
44 Jelinek D *et al*: Identification of a global gene expression signature of B-chronic lymphocytic leukemia. Mol Cancer Res *1*: 346-361, 2003.
45 Klein U *et al*: Gene expression profiling of B cell chronic lymphocytic leukemia reveals a homogeneous phenotype related to memory B cells. J Exp Med *194*: 1625-1638, 2001.
46 Hasko G, Szabo C, Nemeth ZH, Kvetan V, Pastores SM and Vizi ES: Adenosine receptor agonists differentially regulate IL-10, TNF-alpha, and nitric oxide production in RAW 264.7 macrophages and in endotoxemic mice. J Immunol *157*: 4634-40, 1996.
47 Sadikot R *et al*: p47^{phox} Deficiency impairs NF- [{kappa}] B activation and host defense in *Pseudomonas.* Pneumonia *172*: 1801-1808, 2004.
48 Gorlach A *et al*: A p47-phox psuedogene carries the most common mutation causing p-47-phox-deficient chronic granulomatous disease. J Clin Invest *100*: 1907-1918, 1997.
49 Harbord M, Hankin A, Bloom S and Mitchison H: Association between p47^{phox} pseudogenes and inflammatory bowel disease. Blood *101*: 3337, 2003.
50 Kitagawa N *et al*: Epstein-Barr virus-encoded poly(A)- RNA supports Burkitt's lymphoma growth through interleukin-10 induction. EMBO J *19*: 6742-6750, 2000.
51 Chetty M, Thrasher A, Abo A and Casimir C: Low NADPH oxidase activity in Epstein-Barr-virus-immortalized B-lymphocytes is due to a post-transcriptional block in expression of cytochrome b558. Biochem J *306*: 141-145, 1995.
52 Voss T *et al*: Correlation of clinical data with proteomics profiles in 24 patients with B-cell chronic lymphocytic leukemia. Int J Cancer *91*: 180-86, 2001.

Received September 9, 2004
Accepted October 20, 2004